ISSN PRINT 2319 1775 Online 2320 7876

Research paper UGC CARE Listed (Group -I) Journal Volume 11,S Iss 12, Dec 2022

Supercritical Fluid Evaluation and Extraction of Phenol from Sugarcane Bagasse Pyrolysis Oil

Dr. Nookala Venu

Professor, Department of Electronics and Communication Engineering, Balaji Institute of Technology and Science, Warangal - 506 331, Telangana, India

Corresponding Author Mail id: venunookala@gmail.com

Abstract:

This paper presents a simple method to assess the cost of extracting group of phenols from bio-oil derived from pyrolysis of sugarcane bagasse and the incidental profits by employing by what has herein evolved as Supercritical Fluid Extraction (SFE) technology. Further, cost-cum-profit optimization has been done considering minimization of batch time and enhanced purity as the contributive parameters based on experimental results. However, it is acknowledged that the solute extracted using supercritical carbon dioxide in this process is generally significantly different from solute extracted using other conventional alternatives as regards both purity of, and components in, such other extracts. The extract obtained through SFE route deserves to be recognized as an updated, yet distinct, product vis-a-vis conventional/traditional extracts currently available commercially.

Key words: *Phenol, Profit and cost optimization, Supercritical fluid extraction, sugarcane bagasse pyrolysis oil*

1. Introduction

Supercritical extraction using carbon dioxide as a solvent offers unusual possibilities for the selective extraction, fractionation and purification of the oils due to the possibility of adjusting the composition of the extract by varying the solvent density. Commercial plants for supercritical fluid extraction of natural substances have now been in operation for several years. Manufacturing costs are significantly influenced by the energy requirement. Energy optimization may improve the production economics of existing extraction plants. Supercritical fluid extraction is associated with high investment costs; nowadays, an easy method for technical–economical evaluation of supercritical fluid process is not available [1-5]. Thus, a simple method to estimate the cost of manufacturing of extracts and profit by supercritical fluid technology is presented. The manufacturing costs of group of phenols from sugarcane bagasse pyrolysis oil (SBPO) were estimated using the procedure proposed [6-10]. The quality of the oil extracted through the supercritical fluid extraction route depends on the extraction time. Hence, batch time is optimized for maximum profit. The solute extracted using supercritical carbon dioxide is significantly different from their conventional equivalents. There is, in general, apprehension about the high capital cost for high-pressure extraction equipment with high cost of the technology. Nevertheless, energy costs in this process are lower than those incurred in steam distillation and solvent extraction, which more than offset the high capital costs involved in the supercritical CO_2. The higher capital cost of Supercritical Fluid Extraction (SFE) equipment is often offset by

ISSN PRINT 2319 1775 Online 2320 7876

Research paper UGC CARE Listed (Group -I) Journal Volume 11,S Iss 12, Dec 2022

more complete extraction and the purity of the extract [11-14]. The extraction time to yield the same amount of solute is also very less as compared to the solvent extraction process or steam distillation process.

2. Economic appraisal of phenol extraction from bagasse pyrolysis oil

It was observed from the experimental study that the first noticeable extract from bagasse pyrolysis oil was present at 120 bar pressure. Therefore, the experiments were conducted at 120 bar and 300 bar (maximum possible on the present experimental set-up) and at 333 K. The yield of phenol rich oil for 120 bar and 300 bar was 9 % and 15 % respectively [15-19]. The maximum yield of SFE extracted Sugarcane Bagasse Pyrolysis Oil (SBPO) occurs at 300 bar and 333 K. For economic appraisal of phenol extraction same operating parameters have been considered.

2.1 Estimation of the yield

The model proposed method has been used for the yield estimation of the phenol rich sugarcane bagasse oil. The model was validated for the experimental results obtained at 300 bar pressure and 333 K temperature as mentioned earlier [20-26]. The model parameters obtained by regressing experimental results are shown in Table 1.

Table 1: Model parameters for SBPO at 300 bar and 323 K.

Model Parameter	Phenol rich bagasse oil
y_r	0.005241
A	0.5241
B	0.0000445

2.2 Estimation of the annualized manufacturing cost

The cost of production of the phenol rich oil using SFE is calculated based on the various costs, namely, initial investment cost (capital cost), additional process and operational costs (like for coolant's refrigeration, pumping, reheating, maintenance and repairs, etc. (P&OMR cost), and raw material cost, labor cost, cost for carbon dioxide, cost for utilities, etc. (consumptive costs), (revenue costs being the sum of operational and consumptive costs). Period-wise (annual as considered herein) raw material cost comprises: the price of the material from which the solute is to be extracted, the cost of transportation of the raw and finished products, cost for grinding the raw material to the requisite size, and the cost of any pretreatment of the raw material before feeding. The cost of raw sugarcane bagasse oil obtained through pyrolysis is typically taken as $ 50 per tonne.The annualized (equivalent) cycle cost (ALCC) for the output product (on per unit weight basis times the total weight of the output over the period – annual as already considered) comprises the capital recovery component of the capital cost involved taken together with the annual revenue costs (as defined above). Factors referring to the total investment cost of the commercial plant includes: the cost for two 200 liter extraction columns, a pump, a condenser, and the solvent reservoir besides what all are to be assigned in lieu of revenue cost impinging on successful extraction. For this purpose the following become relevant [27-31]. The solvent is chilled to its liquid state prior to its entry to the liquid pump by a secondary refrigerant system. The heat rejected by the refrigerant system in this chilling process is optimally used to heat the solvent to pre-selected temperature at its later injection stage prior to the extraction

ISSN PRINT 2319 1775 Online 2320 7876

Research paper UGC CARE Listed (Group -I) Journal Volume 11,S Iss 12, Dec 2022

column entrance. The life of the plant is assumed as 20 years (n in Eq.(1)) with no salvage value. The ALCC is calculated as the product of the total investment and the capital recovery factor (CRF).

The discount rate d (fraction or percentage) is assumed as 10% for which CRF is calculated by

$$CRF = \frac{d*(1+d)^n}{(1+d)^n - 1} \quad (1)$$

Where, d is the rate of discount and n is plant life.

$$\text{ALCC} = \text{CRF} \times \text{Plant cost} \quad (2)$$

The cost of the commercial SFE unit is considered $ 12 00 000 (Rosa and Meireles, 2005). The annual labour cost is calculated on the basis two labours per shift, a plant engineer and two skilled technicians. The typical wage for a labour, an engineer and a skilled technician in India is $ 60, $ 300 and $ 100 p.m., respectively. The annual maintenance cost is taken as 10% of the annualized capital cost [32-36]. The energy costs are incurred in (i) compressing liquid CO_2 to the pressure required for effecting extraction (ii) heating this compressed high pressure CO_2 to the required temperature for effecting extraction (iii) at the later process step of heating the expanded stream of loaded CO_2 to effect separation (and collection) of the extract load into the separator and (iv) cooling the deprived CO_2 to liquid phase followed by impelling it through the pump into the storage tank. These energy costs are now discussed referring to the sectional flow diagram shown in Fig.1

Fig.1 shows a conceptual process flow diagram that uses a supercritical fluid as the solvent. Solvent is pressurized through the pump impeller from state 1 to 2 to the requisite pressure for extraction. Assuming overall efficiency (η_p) of pump-motor monobloc system as 0.8 (which may however generally be somewhat lesser), total energy required (W_{21}) in this process, in terms of enthalpies, here and wherever further appropriate, is given as

$$W_{21} = \left(\frac{h_2 - h_1}{\eta_p} \right) \quad (3)$$

ISSN PRINT 2319 1775 Online 2320 7876

Research paper UGC CARE Listed (Group -I) Journal Volume 11,S Iss 12, Dec 2022

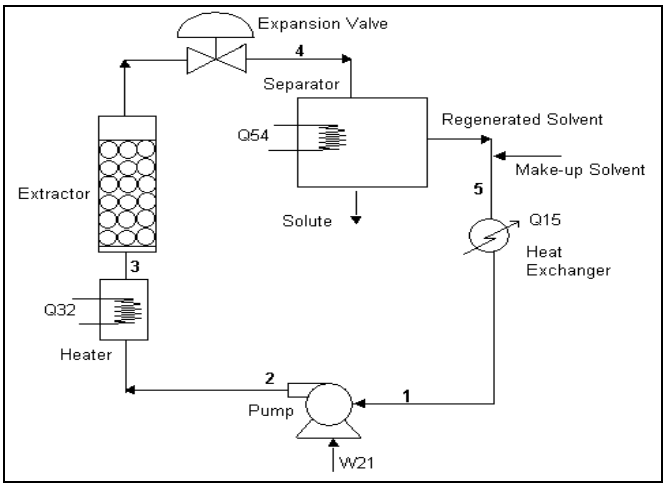

Fig.1 Sectional Schematic Flowchart of the Solvent in SFE Process.

The next process of heating the solvent to the temperature required for extraction (state 3) in the electric heater involves using up of energy W_{32} (equivalent to heat energy Q_{32}) which is given as

$$W_{32} = Q_{32} = (h_3 - h_2) \tag{4}$$

After the instance of extraction, the solute-saturated solvent is depressurized to the tank pressure (state 4) through the expansion valve (without any external energy input), resulting incidentally in cooling of the partially released solute and also the solvent CO_2 to its dry ice phase. This mixture is to be heated by an electric heater to separate the solute from the solvent (state 5). (Total success of the process is mandated on that the solvent so separated from the solute is free from any solute traces.) As was already mentioned, the regenerated solvent is then cooled in the refrigerating unit (heat exchanger) to flow into the impeller inlet in the pump, thus initiating the next cycle.

The energy required by the electric heater (W_{54}) is given as

$$W_{54} = Q_{54} = (h_5 - h_4) \tag{5}$$

The energy associated with the refrigerating unit (W_{15}) is written as

$$W_{15} = \left(\frac{h_5 - h_1}{COP} \right) \tag{6}$$

Where *COP* is the co-efficient of performance of a refrigerating system.

Reading the above energy requirements additively, the total energy consumption (W) in this process is

$$W = W_{21} + W_{32} + W_{54} + W_{15} \tag{7}$$

As declared already, h_1, h_2, h_3, h_4, and h_5 are the respective state-specific enthalpies of the solvent. For computational applications, the specific enthalpies of carbon dioxide in the supercritical and liquid regions respectively were developed separately by regression analyses recounted from property tables of CO_2 as:

ISSN PRINT 2319 1775 Online 2320 7876

Research paper UGC CARE Listed (Group -I) Journal Volume 11,S Iss 12, Dec 2022

for supercritical region (100 to 350 bar pr., 300 to 340 K temp., AARD $\leq$ 1.5%):

$$h = -769.6343 + 3.5161T + 1.6999P - 0.006723PT - 0.0008726P^2 + 4.9516\times10^{-6}TP^2 \quad (8)$$

and, for liquid region (40 to 200 bar pr., 270 to 300 K temp., AARD $\leq$ 2.0%):

$$h = -524.67 + 2.6635T + 0.6545P - 0.002810PT + 0.0003P^2 - 7.28\times10^{-8}TP^2 \quad (9)$$

Equations (8) and (9) have been developed to assist as robust inputs in programmed computations.

We next consider the make-up cost of the solvent. The incidence in this cost is predicated as under. During unloading the post-extraction adscititious residue from the extractor after each run, it becomes inevitable that the remnant solvent in the extractor, which by now has to be brought down to the tank pressure to prevail at 40 bar, has to be discarded and same amount of solvent has to be replenished from make-up system (preceding stage 5 – refer Fig.1). The requisite amount of solvent to replenish to the volume of the extractor (400 liters in this study) is calculated on the basis of the solvent density at this tank pressure. The cost of solvent is taken as $ 0.1 per kg as sourced from M/S Sicgil Corporation, Bombay. The next component, namely, cost of electricity is taken as $ 0.1 per kWh.

2.3 Scaling-up for industrial production

Model developed in the previous section is used for the scale-up estimates. Numerical magnitude of the model parameters (yr, A and B) characterized in the derivation of model equations are obtained from the data of the laboratory unit. Pertinently, the derivation of the equations is immanently equally applicable irrespective of the scale of the production set-up [37-41]. “Industrial scale unit should have the same performance as that of laboratory scale unit for the same particle size, same bed density and the same ratio between the mass of the solid and the solvent flow rate”, read from (Rosa and Mireles, 2005) adduces in this context. The ratio between the mass of particles in the extractor and solvent mass flow rate in the laboratory experimental set-up was 193 seconds. The CO_2 mass flow rate to be used in the industrial production prototype extraction unit can be calculated by dividing this 193 [kg of particles × s/ kg of solvent] with the weight of intended prototype production feed. The overall production mass together with its production time of the prototype can be estimated by this methodology of scaling-up.

2.4 Profit optimization

The data represented in earlier section have already been referred to in this context which highlight that 300 bar is best adopted. The selling cost of the product is taken as the existing cost of petro-based phenols in the market (4 $ per kg). The quantification mentioned here is now explained extended to scaled-up industrial production.

2.5 Computation of profit and identification of profit maximization

Very simply, the annualized profit will be the amount by which the annual sold price income exceeds the total annualized cost of production, this last item being the sum of annualized first cost of plant including erection and commissioning, annual material an labour costs in respect of raw material cost as delivered at site, preparation of raw material to size and pretreatment, plant operation cost including incidental refrigeration, heating and pumping, etc., cost of solvent, man power cost of all descriptions, annual maintenance and repairs and energy costs. These

ISSN PRINT 2319 1775 Online 2320 7876

Research paper **© 2012 IJFANS. All Rights Reserved, UGC CARE Listed (Group -I) Journal Volume 11,S Iss 12, Dec 2022**

have been individually described already. (Depreciation on equipment, disposal of wastes, office and overhead costs, packaging labeling and marketing costs, rentals, etc. may need consideration though not considered here. Considering depreciation would amount to double-counting after having considered animalization of the plant's initial cost [42-48]. The other items would need to be factored into and set out against the profit and hence emphasize the obligation to maximize the profit.) Based on the scaled-up computations cogently with the experimental data from the laboratory set-up, the two graphs shown in Fig.2 have been developed relating each of cost of production and also annualized profit to the extraction time run for each feed.

The profile of the profit curve bears out the discussion in the previous section. At the left hand of the curve the quantity of the extract being small, the profit is hedged notwithstanding the high purity of the extract. Also to be aware of at the left hand of the curve is the fact that the raw material cost as a proportion within the total manufacturing cost is high and, with the quantity extracted being small, the manufacturing cost in its totality is also high. On the other hand, the labour and other utility costs for the smaller extraction durations are proportionately smaller. The opposite influences gain in importance with increase in extraction time. These are demonstrated in Fig.3. Moreover, the profit improves to a maximum at the extraction time of 2.24 h. Though the profit values are nearly the same for extraction times 1.92 and 2.56 and does not increase significantly either in the experimental data range, cost minimization suggests that run time just around 2.24 h is best recommended [49-54]. However to capture as much as possible the extracted oil content, run time up to 2.56 h can be recommended for improving commercial viabilities [55-59]. In addition to employing net profit as a criterion for optimal run time for adherence in prototype production, the internal rate of return (IRR) was also computed for this optimal run time to ward off any bias in the net profit criterion [60-63].This optimal run duration with its annual profit of 81,300 dollar results in an IRR of nearly 19% which shows a good comfort level [64-66].

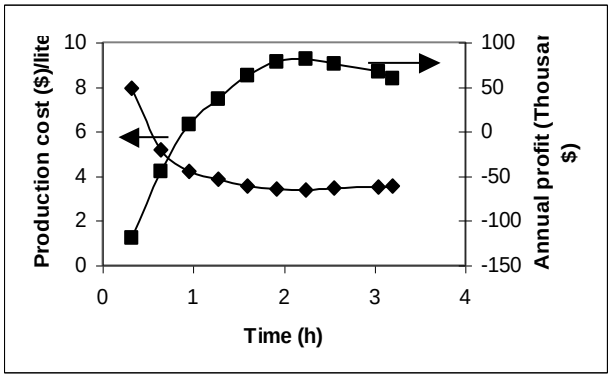

Fig 2: Variation of SBPO cost and annual Profit

ISSN PRINT 2319 1775 Online 2320 7876

Research paper UGC CARE Listed (Group -I) Journal Volume 11,S Iss 12, Dec 2022

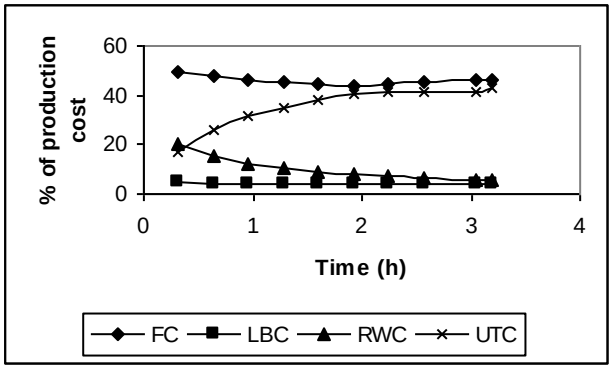

Fig. 3 Influence of different cost components on manufacturing of SBPO

3. Conclusion

Benchmark studies establish that further investigation for extraction of SBPO the other essentials like costs, selling prices and profits shall be based on working conditions of 300 bar, 333 K. Optimum extraction time for these products per run are technologically as well as commercially most economical and profitable. With the annualized cost of the plant inclusive of its installation being by far the largest component in the total cost of extraction, multiple shifts and near continuous working of the plant should be ideally pursued. The optimum extraction time is nearly twice the lower breakeven time and just nearly half the higher breakeven time as seen from Fig.1 and 2, conforming to comparable conditions in the broad spectrum of several industries. The IRR of 19% for extracts from SBPO shows the economic viability of the extraction of such chemicals from biomasses through SFE route. Since the monetary computations are based on 2005-2006 basis in Indian rupees, appropriate quantitative changes in the costs, profit, proportion of profit, and magnitude of IRR may be called for. Sensitivity analyses may further be done in terms of the individual cost components.

References

[1] Nookala Venu, S. K. (2022). Machine Learning Application for Medicine Distribution Management System. IJFANS, 11 (1), 2323-2330.

[2] Vaigandla, K. K., & Venu, D. N. (2021). A survey on future generation wireless communications-5G: multiple access techniques, physical layer security, beamforming approach. *Journal of Information and Computational Science*, *11*(9), 449-474.

[3] Venu, D., Arun Kumar, A., & Vaigandla, K. K. (2022). Review of Internet of Things (IoT) for Future Generation Wireless Communications. *International Journal for Modern Trends in Science and Technology*, *8*(03), 01-08.

[4] Sujith, A. V. L. N., Swathi, R., Venkatasubramanian, R., Venu, N., Hemalatha, S., George, T., ... & Osman, S. M. (2022). Integrating nanomaterial and high-performance fuzzy-based machine learning approach for green energy conversion. *Journal of Nanomaterials*, *2022*, 1-11.

[5] Venu, N., & Anuradha, B. (2013, December). Integration of hyperbolic tangent and Gaussian kernels for fuzzy C-means algorithm with spatial information for MRI segmentation. In *2013 Fifth International Conference on Advanced Computing (ICoAC)* (pp. 280-285). IEEE.

[6] Vaigandla, K. K., & Venu, D. N. (2021). Ber, snr and papr analysis of ofdma and sc-fdma. GIS Science Journal, ISSN, (1869-9391), 970-977.

ISSN PRINT 2319 1775 Online 2320 7876

Research paper UGC CARE Listed (Group -I) Journal Volume 11,S Iss 12, Dec 2022

[7] Venu, N. (2014, April). Performance and evalution of Guassian kernals for FCM algorithm with mean filtering based denoising for MRI segmentation. In *2014 International Conference on Communication and Signal Processing* (pp. 1680-1685). IEEE.

[8] Vaigandla, K. K., & Venu, D. (2021). Survey on Massive MIMO: Technology, Challenges, Opportunities and Benefits.

[9] Venu, N., & Anuradha, B. (2015). Multi-Kernels Integration for FCM algorithm for Medical Image Segmentation Using Histogram Analysis. *Indian Journal of Science and Technology*, *8*(34), 1-8.

[10] Venu, N., Yuvaraj, D., Barnabas Paul Glady, J., Pattnaik, O., Singh, G., Singh, M., & Adigo, A. G. (2022). Execution of Multitarget Node Selection Scheme for Target Position Alteration Monitoring in MANET. *Wireless Communications and Mobile Computing*, *2022*.

[11] Venu, N., Swathi, R., Sarangi, S. K., Subashini, V., Arulkumar, D., Ralhan, S., & Debtera, B. (2022). Optimization of Hello Message Broadcasting Prediction Model for Stability Analysis. *Wireless Communications & Mobile Computing (Online)*, *2022*.

[12] Venu, D. N. Analysis of Xtrinsic Sense MEMS Sensors. *International Journal of Advanced Research in Electrical, Electronics and Instrumentation Engineering (IJAREEIE), ISSN*, 2278-8875.

[13] Venu, N., & Anuradha, B. (2013). A novel multiple-kernel based fuzzy c-means algorithm with spatial information for medical image segmentation. *International Journal of Image Processing (IJIP)*, *7*(3), 286.

[14] Nookala Venu, A. (2018). Local mesh patterns for medical image segmentation. *Asian Pacific Journal of Health Sciences*, *5*(1), 123-127.

[15] Venu, N., & Anuradha, B. (2013). PSNR Based Fuzzy Clustering Algorithms for MRI Medical Image Segmentation. *International Journal of Image Processing and Visual Communication*, *2*(2), 01-07.

[16] Thouti, S., Venu, N., Rinku, D. R., Arora, A., & Rajeswaran, N. (2022). Investigation on identify the multiple issues in IoT devices using Convolutional Neural Network. *Measurement: Sensors*, *24*, 100509.

[17] Venu, N., Revanesh, M., Supriya, M., Talawar, M. B., Asha, A., Isaac, L. D., & Ferede, A. W. (2022). Energy Auditing and Broken Path Identification for Routing in Large-Scale Mobile Networks Using Machine Learning. *Wireless Communications and Mobile Computing*, *2022*.

[18] Kesavaiah, D. C., Goud, T. R., Rao, Y. S., & Venu, N. (2019). Radiation effect to MHD oscillatory flow in a channel filled through a porous medium with heat generation. *Journal of Mathematical Control Science and Applications*, *5*(2), 71-80.

[19] Venu, N., & Anuradha, B. (2015). Medical Image Segmentation Using Kernal Based Fuzzy C Means Algorithm. *Research Scholar, Dept. of ECE, SVU College of Engineering, Sri Venkateswara University, Tirupati-517502, India*, *4*(1).

[20] Nookala Venu, D., Kumar, A., & Rao, M. A. S. (2022). BOTNET Attacks Detection in Internet of Things Using Machine Learning. *Neuroquantology*, *20*(4), 743-754.

[21] Venu, N., & Anuradha, B. (2014, February). Multi-Hyperbolic Tangent Fuzzy C-means Algorithm for MRI Segmentation. In *Proceedings of International Conference on Advances in Communication, Network and Computing (CNC-2014), Elsevier* (pp. 22-24).

[22] Nookala Venu, S. W. (2022). A Wearable Medicines Recognition System using Deep Learning for People with Visual Impairment. *IJFANS*, *12*(1), 2340-2348.

[23] Venu, D., Rakesh, G., Maneesha, K., Anusha, K., Merugu, S., & Mohammad, A. (2022). Smart Road Safety and Vehicle Accidents Prevention System for Mountain Road. *International Journal from Innovative Engineering and Management Research (IJIEMR)*.

[24] Nookala Venu, D., Kumar, A., & Rao, M. A. S. (2022). Smart Agriculture with Internet of Things and Unmanned Aerial Vehicles. *Neuroquantology*, *20*(6), 9904-9914.

ISSN PRINT 2319 1775 Online 2320 7876

Research paper **© 2012 IJFANS. All Rights Reserved,** UGC CARE Listed (Group -I) Journal Volume 11,S Iss 12, Dec 2022

[25] Nookala Venu, D., Kumar, A., & Rao, M. A. S. (2022). Internet of Things Based Pulse Oximeter For Health Monitoring System. *NeuroQuantology*, *20*(5), 5056-5066.

[26] Venu, D. N. DA (2021). Comparison of Traditional Method with watershed threshold segmentation Technique. *The International journal of analytical and experimental modal analysis*, *13*, 181-187.

[27] Vaigandla, K. K., & Venu, D. (2021). Survey on Massive MIMO: Technology. *Challenges, Opportunities and Benefits*.

[28] Kesavaiah, D. C., Goud, T. R., Venu, N., & Rao, Y. S. (2021). MHD Effect on Convective Flow Of Dusty Viscous Fluid With Fraction In A Porous Medium And Heat Generation. *Journal of Mathematical Control Science and Applications*, *7*(2).

[29] Babu, K. R., Kesavaiah, D. C., Devika, B., & Venu, D. N. (2022). effect on MHD free convective heat absorbing Newtonian fluid with variable temperature. *NeuroQuantology*, *20*(20), 1591-1599.

[30] Kesavaiah, D. C., Ahmed, M., Reddy, K. V., & Venu, D. N. (2022). Heat and mass transfer effects over isothermal infinite vertical plate of Newtonian fluid with chemical reaction. *NeuroQuantology*, *20*(20), 957-967.

[31] Reddy, G. B., Kesavaiah, D. C., Reddy, G. B., & Venu, D. N. (2022). A note on heat transfer of MHD Jeffrey fluid over a stretching vertical surface through porous plate. *NeuroQuantology*, *20*(15), 3472-3486.

[32] Chenna Kesavaiah, D., Govinda Chowdary, P., Rami Reddy, G., & Nookala, V. (2022). Radiation, radiation absorption, chemical reaction and hall effects on unsteady flow past an isothermal vertical plate in a rotating fluid with variable mass diffusion with heat source. *NeuroQuantology*, *20*(11), 800-15.

[33] Kesavaiah, D. C., Prasad, M. K., Reddy, G. B., & Venu, N. (2022). Chemical Reaction, Heat and Mass Transfer Effects on MHD Peristaltic Transport in A Vertical Channel Through Space Porosity And Wall Properties. *NeuroQuantology*, , *20*(11), 781-794.

[34] Kesavaiah, D. C., Reddy, G. B., Kiran, A., & Venu, D. N. (2022). MHD effect on boundary layer flow of an unsteady incompressible micropolar fluid over a stretching surface. *NeuroQuantology*, , *20*(8), 9442-9452.

[35] Kesavaiah, D. C., Chowdary, P. G., Chitra, M., & Venu, D. N. (2022). Chemical reaction and MHD effects on free convection flow of a viscoelastic dusty gas through a semi infinite plate moving with radiative heat transfer. *NeuroQuantology*, *20*(8), 9425-9434.

[36] Karne, R., Mounika, S., & Venu, D. (2022). Applications of IoT on Intrusion Detection System with Deep Learning Analysis. *International Journal from Innovative Engineering and Management Research (IJIEMR)*.

[37] Venu, N., & Anuradha, B. (2015). Two different multi-kernels for fuzzy C-means algorithm for medical image segmentation. *Int. J. Eng. Trends Technol.(IJETT)*, *20*, 77-82.

[38] Kesavaiah, D. C., Goud, T. R., Venu, N., & Rao, Y. S. (2017). Analytical Study on Induced Magnetic Field With Radiating Fluid Over A Porous Vertical Plate With Heat Generation. *Journal of Mathematical Control Science and Applications*, *3*(2).

[39] Venu, N., & Kumar, A. A. Routing and Self-Directed Vehicle Data Collection for Minimizing Data Loss in Underwater Network.

[40] Venu, N., & Kumar, A. A. Fuzzy Based Resource Management Approach for the Selection Of Biomass Material.

[41] Agarwal, R. K., Sahasrabuddhe, D., & Riyajuddin, A. A Novel Dates Palm Processing and Packaging Management System based on IoT and Deep Learning Approaches.

[42] Koshariya, A. K., Rout, S., & Venu, N. An Enhanced Machine Learning Approach for Identifying Paddy Crop Blast Disease Management Using Fuzzy Logic.

[43] Rout, S., & Venu, N. Machine Learning Based Analysis And Classification of Rhizome Rot Disease In Turmeric Plants.

ISSN PRINT 2319 1775 Online 2320 7876

Research paper **© 2012 IJFANS. All Rights Reserved, UGC CARE Listed (Group -I) Journal Volume 11,S Iss 12, Dec 2022**

[44] Jagadeesan, S., Barman, B., Agarwal, R. K., Srivastava, Y., Singh, B., Nayak, S. K., & Venu, N. A Perishable Food Monitoring Model Based on Iot And Deep Learning To Improve Food Hygiene And Safety Management. *interventions*, *8*, 9.

[45] Venu, N., Thalari, S. K., Bhat, M. S., & Jaiganesh, V. Machine Learning Application for Medicine Distribution Management System.

[46] Reddy, A. V., Kumar, A. A., Venu, N., & Reddy, R. V. K. (2022). On optimization efficiency of scalability and availability of cloud-based software services using scale rate limiting algorithm. *Measurement: Sensors*, *24*, 100468.

[47] Venu, D. (2022). Radiation Effect to Mhd Oscillatory Flow in a Channel Filled Through a Porous Medium with Heat Generation. *Radiation Effect to Mhd Oscillatory Flow in a Channel Filled Through a Porous Medium with Heat Generation (August 27, 2022). Research Article*.

[48] Venu, N. Smart Agriculture Remote Monitoring System Using Low Power IOT Network.

[49] Venu, N. IOT Surveillance Robot Using ESP-32 Wi-Fi CAM & Arduino.

[50] Venu, D., Soujanya, N., Goud, B. M., Bhavani, T. Y., & Rajashekar, A. (2022). Study and Experimental Analysis on FBMC and OFDM. *International Journal from Innovative Engineering and Management Research (IJIEMR)*.

[51] Katti, S. K., Ananthula, A., & Venu, D. (2022). Vehicle Fuel Level Monitor and Locate the Nearest Petrol Pumps Using IoT.

[52] Priya R, S., Tahseen, A., & Venu, D. (2022). Face Mask Detection System Using Python Open CV.

[53] Venu, D. (2022). Alcohol Detection and Engine Locking System. *International Journal from Innovative Engineering and Management Research (IJIEMR)*.

[54] Venu, D., Bindu, C., Srija, B., Maheshwari, V., Sarvu, S., & Rohith, S. (2022). Wireless Night Vision Camera on War Spying Robot. *International Journal from Innovative Engineering and Management Research (IJIEMR)*.

[55] Venu, N. IOT Based Enabled Parking System in Public Areas.

[56] Venu, N. IOT Based Speech Recognition System to Improve the Performance of Emotion Detection.

[57] Venu, N., & Sulthana, M. A. Local Maximum Edge Binary Patterns for Medical Image Segmentation.

[58] Venu, N. Design and intergration of different kernels for fuzzy means algorithm used for MRI medical image segmentation.

[59] Venu, N., & Anuradha, B. (2016). Multi-hyperbolic tangent fuzzy c-means algorithm with spatial information for MRI segmentation. *International Journal of Signal and Imaging Systems Engineering*, *9*(3), 135-145.

[60] Venu, N., & Anuradha, B. (2015). Hyperbolic Tangent Fuzzy C-Means Algorithm with Spatial Information for MRI Segmentation. *International Journal of Applied Engineering Research*, *10*(7), 18241-18257.

[61] Venu, N., & Anuradha, B. (2015, April). Two different multi-kernels integration with spatial information in fuzzy C-means algorithm for medical image segmentation. In *2015 International Conference on Communications and Signal Processing (ICCSP)* (pp. 0020-0025). IEEE.

[62] Venu, N., & Anuradha, B. (2015). MRI Image Segmentation Using Gaussian Kernel Based Fuzzy C-Means Algorithm.

[63] Venu, N., & Anuradha, B. (2015). Evaluation of Integrated Hyperbolic Tangent and Gaussian Kernels Functions for Medical Image Segmentation. *International Journal of Applied Engineering Research*, *10*(18), 38684-38689.

[64] Anita Tuljappa, V. N. (2022). Dufour and Chemical Reaction Effects on Two Dimensional incompressible flow of a Viscous fluid over Moving vertical surface. *NeuroQuantology* , 63-74.

[65] Ch. Achi Reddy, V. N. (2022). Magnetic Field And Chemical Reaction Effects on Unsteady Flow Past A Stimulate Isothermal Infinite Vertical Plate. *NeuroQuantology* , *20* (16), 5360- 5373.

ISSN PRINT 2319 1775 Online 2320 7876

Research paper **UGC CARE Listed (Group -I) Journal Volume 11,S Iss 12, Dec 2022**

[66] Sowmya Jagadeesan, M. K. (2022). Implementation of an Internet of Things and Machine learning Based Smart Medicine Assistive System for Patients with Memory Impairment. *IJFANS International Journal of Food and Nutritional Sciences* , 1191-1202.